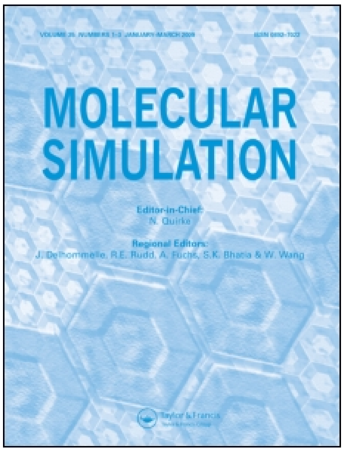

Molecular Simulation
Publication details, including instructions for authors and subscription information:
http://www.informaworld.com/smpp/title~content=t713644482

RMDff: A smoothly transitioning, forcefield-based representation of kinetics for reactive molecular dynamics simulations

K. D. Smith[a]; S. I. Stoliarov[b]; M. R. Nyden[c]; P. R. Westmoreland[a]
[a] Department of Chemical Engineering, University of Massachusetts Amherst, Amherst, MA, USA [b] SRA International Inc., Egg Harbor Township, NJ, USA [c] Building and Fire Research Laboratory, National Institute of Standards and Technology, Gaithersburg, MD, USA

To cite this Article Smith, K. D. , Stoliarov, S. I. , Nyden, M. R. and Westmoreland, P. R.(2007) 'RMDff: A smoothly transitioning, forcefield-based representation of kinetics for reactive molecular dynamics simulations', Molecular Simulation, 33: 4, 361 — 368

To link to this Article: DOI: 10.1080/08927020601156392

URL: http://dx.doi.org/10.1080/08927020601156392

Molecular Simulation, Vol. 33, Nos. 4–5, 15–30 April 2007, 361–368

Taylor & Francis
Taylor & Francis Group

RMDff: A smoothly transitioning, forcefield-based representation of kinetics for reactive molecular dynamics simulations

K. D. SMITH†§, S. I. STOLIAROV‡||, M. R. NYDEN¶# and P. R. WESTMORELAND†*

†Department of Chemical Engineering, University of Massachusetts Amherst, Amherst, MA 01003, USA
‡SRA International Inc., 3120 Fire Road, Egg Harbor Township, NJ 08234, USA
¶Building and Fire Research Laboratory, National Institute of Standards and Technology, 100 Bureau Drive, Gaithersburg, MD 20899, USA

(Received June 2006; in final form November 2006)

RMDff is a new forcefield that smoothly couples the reactive intersections of potential energy surfaces to model chemical reactions. The method uses switching functions to accomplish a smooth transition from reactant to product atom types. This paper demonstrates and tests RMDff for homolytic scissions. The reaction networks are described by localized events involving only a few atoms, so that the complex mechanisms employed in conventional kinetics modeling are not needed. Unlike quantum chemical calculations, which are feasible only for small molecules, this new valence-bond forcefield can be coupled with Reactive Molecular Dynamics to describe chemical reactions in large domains.

Keywords: Molecular dynamics; Forcefields; Reactive forcefield; Kinetics; Homolysis

1. Introduction

A fundamental, microscopic understanding of kinetics in polymer decomposition cannot be obtained using current experimental techniques. Understanding of these phenomena would provide useful insights into many chemical processes, such as materials flammability. The "Reactive Molecular Dynamics" (RMD) method of Nyden *et al.* [1–5] allows investigation of the microscopic reactive environment. It couples forcefield molecular dynamics with an algorithm that describes chemically reactive trajectories. Although reactive events are rare on the time scale of molecular dynamics, RMD simulations can be run for sufficiently long times to observe individual reactions and the conformational changes that accompany them.

A full molecular-orbital approach would be ideal because it is inherently more accurate and there is no explicit specification of the covalent bonding, but such calculations are impractical for large systems [6,7]. On the other hand, empirical reactive forcefields, such as ReaxFF [8,9] and REBO [10–13] are quite heavily parameterized and not easily tailored to individual situations that might be desired to represent energetics including transition states. Since RMDff requires less parameterization, it represents a compromise solution to the description of chemical reactivity in large molecules and nanostructures.

A valence-bond reactive forcefield was developed for our previous RMD code, MD_React, using a modified version of the consistent valence forcefield (CVFF) [3]. Reactions occur between explicitly bonded and non-bonded atoms. Bonding is thus reevaluated at every time step, and the lowest-energy bonding is selected before execution of the next time step. The intermediate molecular structure must also conform to the following constraints: (i) connectivity to an atom must not exceed unity plus its maximum valence and (ii) the sum of bond orders of all bonded atoms to the central atom must be less than the valence. This model allows for the chemical structure to change throughout the

---

*Corresponding author. Tel.: + 413-545-1750. Fax: + 413-545-1647. Email: westm@ecs.umass.edu
§Tel.: +413-545-2234. Fax: +413-545-1647. Email: ksmith@ecs.umass.edu
||Tel.: +609-485-6500. Fax: +609-485-6909. Email: stanislav.ctr.stoliarov@faa.gov
#Tel.: +301-975-6692. Fax: +301-975-4052. Email: marc.nyden@nist.gov

Molecular Simulation
ISSN 0892-7022 print/ISSN 1029-0435 online © 2007 Taylor & Francis
http://www.tandf.co.uk/journals
DOI: 10.1080/08927020601156392

dynamics, thereby describing the time evolution of reaction products and intermediates.

Our present method uses localized descriptions of reactive events to describe the chemical transitions that occur during a reaction. This approach is derived partially from previous efforts to model transition-state structures from forcefield methods [14–17]. In those studies, several groups have devised methods to determine the minimum energy path between a reactant and product using forcefield representations of the potential energy. Also of note is the work of Truong and coworkers [18,19], who have developed the Reaction Class transition-state theory. This analysis relates the kinetics of reactions for larger molecules to gas-phase reactions of simple molecules. A combination of these two ideas suggests that accurate chemical representations of forcefield-based reactions can be developed and implemented for use in RMD from simple localized valence-bond representations.

The objective of this work is to develop an initial form of RMDff, a chemically accurate, forcefield-based model for representing reactions within a dynamic simulation. RMDff employs a standard equilibrium forcefield representation of the atomic interactions in the vicinity of the equilibrium products, where these forcefields are known to provide adequate chemical accuracy. Switching functions are employed to facilitate smooth transitions between the reactant, transition state and product structures within the context of a complete and generic reactive potential energy surface (PES).

2. Computational details

2.1 Quantum chemical calculations

The *ab initio* calculations for parameterization and comparison were performed using the Gaussian 98 [20] and 03 [21] programs. All geometry optimizations and frequency calculations were completed using the UB3LYP/6-311++G(2d,p) level of theory. The energies of the optimized structures were determined from UCCSD(T)/cc-pVTZ calculations using an initial guess of a mixture of HOMO and LUMO orbitals.

For scission reactions, the geometry was optimized by holding the dissociating bond length fixed and allowing all other modes to relax to equilibrium. The Counterpoise Basis-Set Superposition error was corrected in dissociations by the method of Boys [22]. Changes in zero-point energy were taken into account by a multiplicative factor, scaling the dissociation energy to the value with the zero-point energy correction applied. For carbon-carbon dissociation in ethane, a comparison between the scaled and exact zero-point energy from a UB3LYP/ 6-311++G(2d,p) calculation is applied to the energy calculations shown in figure 1. The change in zero-point energies during homolytic bond dissociations appears to be represented accurately by this approximation.

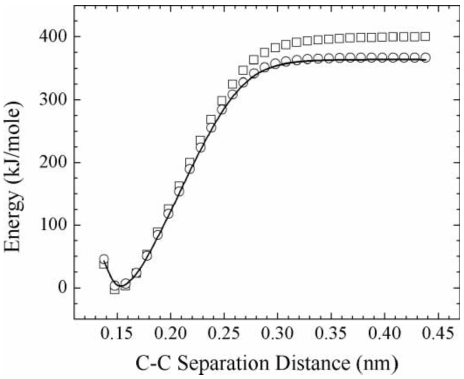

Figure 1. Correcting the energy of C—C dissociation in ethane (□) for the change in zero point energy explicitly by the zero point energy at each geometry (○) and by scaling the dissociation energy (line).

2.2 MM3 forcefield

The MM3 forcefield [23–25] is used to represent the atomic interactions in this study. This forcefield has been demonstrated to provide reasonably accurate results near equilibrium of molecular conformations with an average conformational energy error of 1.5 kJ/mole for hydrocarbons and a total error of 2.6 kJ/mole [26]. Other comparisons of the MM3 forcefield have demonstrated that it is capable of representing a wide range of chemical complexity [27–30].

Parameters for the hydrogen-hydrogen model were not available in the MM3 forcefield, so they were taken from UB3LYP/6-311++G(2d,p) optimization calculations. On the basis of these calculations, the force constant was determined to be 6.59×10^2 N/m and the equilibrium bond distance 0.0744 nm.

3. Results and discussion

3.1 Dissociation of bonds using the MM3 quartic bond potential

The MM3 forcefield uses a quartic bond-stretching potential, which is inadequate for the description of chemical bond dissociation. Consequently, a correction was applied to represent any bond stretches by a hybrid between the MM3 quartic and Morse potentials. At a bond distance greater than r_s, the MM3 quartic bond potential is switched to a Morse-type potential.

In order to ensure continuity and smoothness of the forces, the values of the energy and first and second derivatives of the MM3 quartic and Morse potentials are required to be equal at r_s. Because the parameters of the MM3 quartic potential are used in the vicinity of the equilibrium conformation, there are four parameters to be determined from three equations. The single degree of freedom was chosen to be the dissociation energy, D_E, of the Morse potential. These values were calculated from CBS-QB3 *ab initio* calculation [3] and were corrected for zero-point energy by setting it equal to $\Delta H^{\circ}(T = 0K)$. The parameters of the modified-Morse-potential portion of the composite bond potential are shown in table 1.

3.2 The homolytic scission model

The reaction coordinate (RC) is a measure of the location of the transient structures on the PES relative to the positions of reactant(s) and product(s). For each reaction, a mathematical function for the RC is developed. The forward reaction begins at $\mathrm{RC} = 0$ and ends at $\mathrm{RC} = 1$. Because the reactions are descriptions of the complete PES, the reverse reaction is described by starting at $\mathrm{RC} = 1$ and proceeding to $\mathrm{RC} = 0$.

Reaction potentials were developed initially for simple homolytic scissions. For these reactions, the RC of interest is the bond distance between the dissociating atoms. The RC is represented by a simple linear function,

$$\mathrm{RC} = mr + b \tag{1}$$

where m and b are parameters. The RC parameters are given in table 2 for H—H, C—H and C—C scission reactions. Bounds on the active RC range ($\mathrm{RC} = 0$ and 1) are set to 5 and 99% of the dissociation energy, respectively.

Switching functions are used to transition smoothly between the atom types that describe the reactant(s) and product(s), capturing transitions such as sp^3 to sp^2 hybridization changes in carbon as a bond breaks. In each case, the switching function creates a transition for any forcefield term where a change in atom type is encountered. The switching functions are unity at $\mathrm{RC} = 0$ and transition to zero at $\mathrm{RC} = 1$. A suitable switching function is:

$$S(\mathrm{RC}) = 0.5[1 - \tanh(a(\mathrm{RC} - \mathrm{RC}_0))] \tag{2}$$

where $S(\mathrm{RC})$ is the value of the switching function as a function of RC, a is the steepness parameter, and RC_0 is a parameter such that $S(\mathrm{RC}_0) = 0.5$.

Table 1. Parameters for hybrid quartic/Morse potential[†].

Bonded atoms	*D_E (kJ/mole)*	*α (nm^{-1})*	*r_e (nm)*	*r_s (nm)*
h—h	436.8	18.91	0.0740	0.0871
cg—h	406.3	17.44	0.1108	0.1251
c1—h	394.6	17.77	0.1108	0.1249
c2—h	406.3	17.44	0.1108	0.1251
c3—h	418.0	17.13	0.1108	0.1254
c4—h	433.8	16.73	0.1107	0.1257
cf—h	443.9	17.53	0.1097	0.1240
c—c1	348.5	18.59	0.1522	0.1655
c—c2	353.6	18.42	0.1522	0.1657
c—c3	356.1	18.34	0.1521	0.1657
c—cf	411.7	18.35	0.1496	0.1632
c1—c1	353.6	18.42	0.1522	0.1657
c1—c2	358.6	18.25	0.1521	0.1658
c1—c3	361.1	18.17	0.1521	0.1659
c1—cf	411.7	18.35	0.1496	0.1632
c2—c2	363.6	18.09	0.1521	0.1659
c2—c3	366.1	18.01	0.1521	0.1660
c2—cf	411.7	18.35	0.1496	0.1632
c3—c3	370.3	17.88	0.1521	0.1661
c3—cf	411.7	18.35	0.1496	0.1632

[†] Atom types are defined in table A1.

Table 2. Parameters for HH, CH and CC bond scissions.

Parameter	*HH*	*CC*	*CH*
RC region (nm)	0.085–0.375	0.169–0.393	0.124–0.370
m (nm^{-1})	3.448	4.45	4.07
b	−0.293	−0.752	−0.504
a_1	5.164	14.05	5.50
$\mathrm{RC}_{0,1}$	0.491	0.610	0.502
a_2	–	33.60	19.87
$\mathrm{RC}_{0,2}$	–	0.100	0.299
E_{base} (kJ/mole)	436.8	364.0	401.7

For the simplest case, dissociation of a hydrogen molecule, the energy is given by:

$$E_{H_2\mathrm{Dissociation}} = S(\mathrm{RC})E_{\mathrm{bond}} + [1 - S(\mathrm{RC})](E_{\mathrm{vdw}} + E_{\mathrm{base}}) \tag{3}$$

where E_{bond} is the H_2 bonding potential, E_{vdw} is the van der Waals potential, and E_{base} is the baseline energy value from table 2. A single switching function is used to represent all the atomic changes that occur during dissociation of hydrogen.

The situation is more complicated for dissociation of the C—C and C—H bonds in ethane. In the case of the C—C bond, the carbon atoms change hybridization from sp^3 to sp^2. This transition creates more complexity in the representation of energetics. Thus, as the C—C bond breaks, H—sp^{3}C—H bond angles also transform to H—sp^{2}C—H bond angles. The H—sp^{3}C—sp^{3}C bond angles and H—sp^{3}C—sp^{3}C—H torsions are smoothly turned off because these constraints are not longer active in the resulting methyl radicals. At the same time, necessary non-bonded interactions are turned on. A similar set of changes occurs when the C—H bond dissociates, except only one of the carbon atoms changes hybridization. In larger molecules, any atom with connectivity to another atom that alters its bonding would also be included. For example, if the central C—C bond underwent a scission reaction in n-decane, a C—C—C—C torsional motion (plus H—C—C—C and H—C—C—H torsions, two C—C—C and multiple H—C—H, H—C—C bond angles) would also be turned off, as well as the non-bonded interactions turned on.

Two switching functions, denoted as S_1 and S_2, are needed to yield an accurate description of the changes in the PES accompanying the C—C and C—H bond scissions in ethane. S_1 is used to model all bonded and non-bonded interactions. It is also used for the transformation of any angular or torsional terms that do not contain both of the dissociating atoms. S_2 is used to model the transition of any angular or torsional term that contains both dissociating atoms. Although both switching functions depend on the same RC, they have different values of a and RC_0. S_1 is a more gradual transition, while S_2 is a much quicker transition occurring very early in the dissociation process. The distinction between the modes associated with S_1 and S_2 is supported by changes observed in the geometries obtained from quantum chemical calculations.

The energetics of the fits obtained for H—H dissociation in hydrogen and C—C and C—H dissociation in ethane are shown in figure 2, and the switching functions are shown in figure 3. Good agreement between the *ab initio* calculations and the reactive forcefield is obtained, although there is a slight non-monotonic deviation for C—C scission (figure 2b). The use of the complete and smooth PES allows this method to conserve energy. Because the value of E_{base} is tracked throughout the simulations, energy is conserved even once a reaction is completed. Therefore, the method is accurate for use in NVE as well as thermostatted and barostatted calculations.

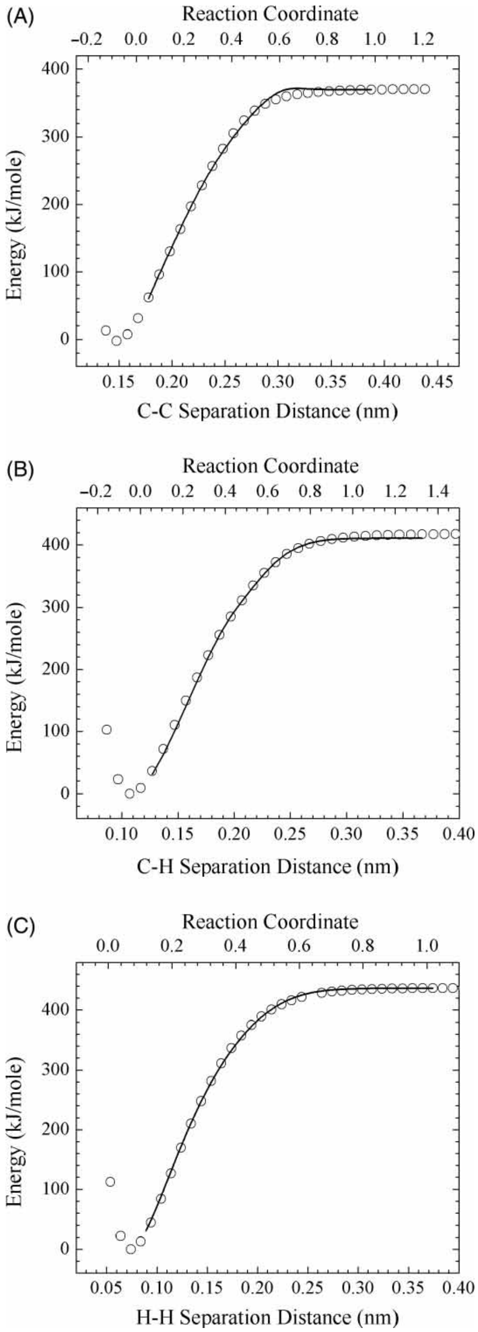

Figure 2. Fits of (a) H—H, (b) C—C and (c) C—H dissociation energy models (lines) to *ab initio* data (circles).

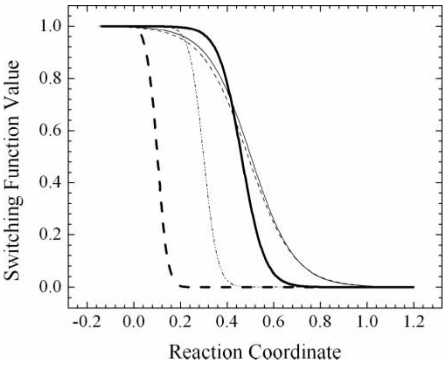

Figure 3. Switching function versus RC for H—H dissociation (dashed line), C—C S_1 switching function (thick line) and C—C S_2 switching function (thick dashed line), and C—H S_1 switching function (thin line) and C—H S_2 switching function (dash-dot line).

According to transition-state theory, the rate constant depends on the rate of changes in the vibrational frequencies of the reacting molecule. Therefore, if the reactive forcefield is expected to give an accurate description of reaction kinetics, it must also do a reasonable job representing force constants throughout the reactive phase space. Frequencies of the vibrational modes of ethane were calculated by normal mode analysis of the reactive forcefield with the slope of the PES projected out. The structures were analyzed along the minimum-energy path of the quantum chemical calculations, based on the assumption that these geometries provide a reasonably close approximation to the minimum-energy path of the reactive forcefield. Only those modes which underwent significant changes are shown in figure 4.

Good agreement between the forcefield and *ab initio* results was obtained for the C—H frequencies corresponding to the static modes, which are not displayed. A comparison between the frequencies derived from the forcefield and those from quantum chemical calculations indicate that the forcefield tends to underestimate the actual frequencies. This is not surprising because, the MM3 forcefield appears to underestimate the frequencies of equilibrium ethane as shown in table 3. The switching functions may actually cause some modes to be completely turned off prior to the complete dissociation of the associated modes. Several modes are still present in the *ab initio* frequencies even as the reaction approaches RC = 1. Therefore, the forcefield may represent the modes too loosely and could result in increased kinetic rates compared to the results expected from *ab initio* calculations. A significant jump in some frequencies occur near $\mathrm{RC}_{0,1}$, where the meshing of the two forcefield terms transition from bonded to non-bonded interactions.

A series of random geometric distortions were introduced at random points along the minimum energy path to test the robustness of the forcefield. Deviations were kept small to prevent additional RC's from becoming active. The average variation in the bond lengths was approximately ±0.005 nm, while average deviations of the bond angles and torsions were about ±5°. Energies from the forcefield are compared to values obtained from the quantum calculations in figure 5. The forcefield tends to

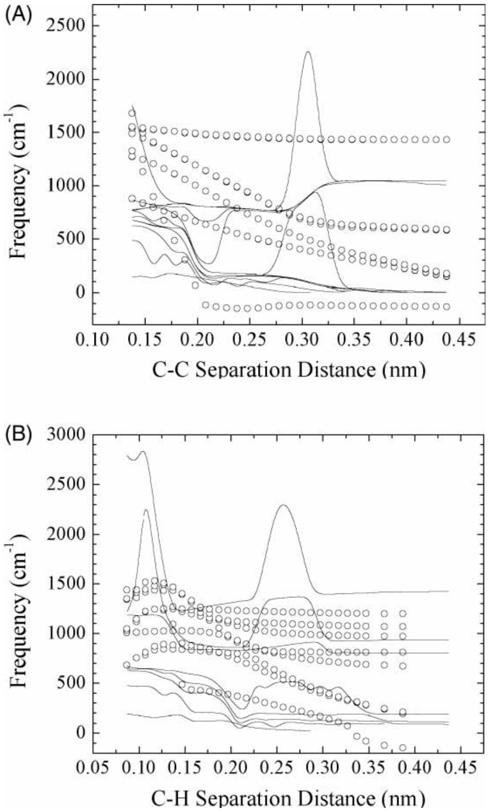

Figure 4. Frequencies obtained from the reactive potential using MM3 (lines) and the frequencies from UB3LYP/6-31G(d) calculations for (a) C—C and (b) C—H bond dissociation in ethane.

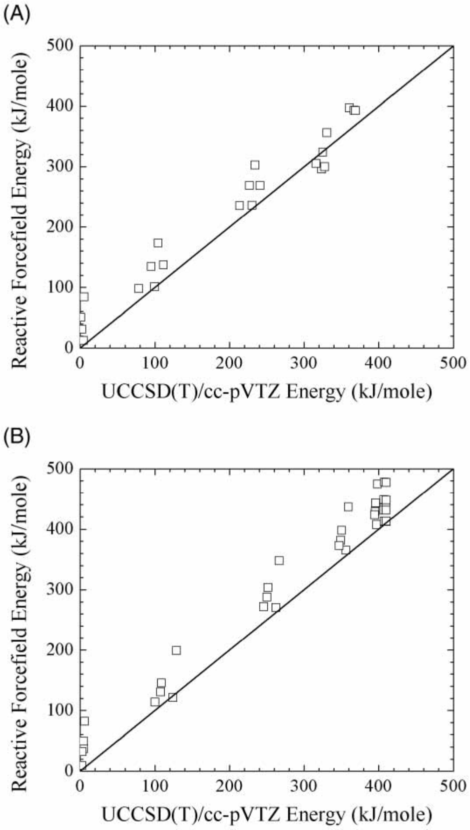

Figure 5. Calculated energy as compared to *ab initio* energy for randomly distorted structures near the bond scission minimum energy path for (a) C—C scission and (b) C—H scission.

over-predict the *ab initio* energy by about 40 kJ/mole for C—H bond scission and 45 kJ/mole C—C for bond scission. This over-prediction in energy appears to be independent of the RC. In figure 5(a), a notable distribution of forcefield energy is observed at a quantum chemical energy of 0 kJ/mole. These deviations reflect those of the MM3 forcefield alone, as the C—C bond is not yet stretched sufficiently to cause the reactive potential to be active. Therefore, the deviations observed are the result of the MM3 forcefield description.

Table 3. Comparison of equilibrium ethane frequencies (cm^{-1}) from *ab initio* and MM3 calculations.

UB3LYP/6-31G(d)	*MM3*
304	164
825	516
826	521
993	647
120	647
1221	721
1410	795
1422	796
1502	830
1503	832
1505	836
1505	1187
3025	2973
3068	2994
3068	3050
3094	3111
3094	3115
3204	3115

3.3 Testing transferability of the model

Dissociations of C—C and C—H bonds were tested in other molecules to examine the transferability of the reactive forcefield parameters. In each case, the RC and switching-function parameters listed in table 2 were used to model the scission reactions. It is important to note that the value of E_{base} represents the forcefield-based dissociation energy for the molecular structure of interest. Although the MM3 potential contains a radical carbon atom type, it is parameterized for hydrocarbon species as opposed to the compounds we tested, which contain hetero-atoms. Because the radical carbon and alkene sp^2 carbon types for hydrocarbons are similar with respect to bond angles and torsions, we assumed that they would provide a reasonable approximation to the radical carbon types for CHX species.

The switching functions, parameterized by our calculations of the dissociation of the C—C bond in ethane, were compared for propane, fluoroethane and ethyl amine (figure 6a–c), while the switching functions obtained from the calculations of the C—H bond dissociation in ethane were compared for methane, methanol and acetaldehyde (figure 6d–f). In general, the model appears transferable to a variety of species.

The main source of error appears to be description of the radicals (i.e. the simplified treatment of the radical carbon type), as opposed to the switching function parameters. The errors were small when minor substitutions were made to the base chemical structure, but larger deviations were observed for non-alkanes. For example, the forcefield energy over-predicted the energy of acetaldehyde (H—CH_2CHO). This is not surprising because CH_2CHO is resonance-stabilized and is not well described by a simple sp^2 radical carbon atom. For ethylamine, the use of the switching function causes the potential energy to overshoot the MM3 energy of the dissociated radical by about 7 kJ/mole. While it is possible that use of larger a in the switching function would force the PES curve down, it may also be that the evolving radical is resonance-stabilized by the lone pair on the nitrogen atom [31,32]. In any case, it appears likely that a more accurate model representation could be obtained by adjusting the forcefield parameters to provide a better description of the radical species.

4. Conclusions

A valence-bond representation of chemical reactions for hydrocarbon systems, which we call RMDff, was introduced in this paper. Accurate and smooth PES's for scission reactions were obtained through the use of switching functions that allow the atom types in the reactant and product to change with the chemical bonding. Good agreement between the forcefield and *ab initio* PES was demonstrated for bond scission reactions in hydrogen and ethane. A comparison to other molecules reveals that the parameters are transferable, with some slight deviations due to the use of non-optimal parameters for the description of

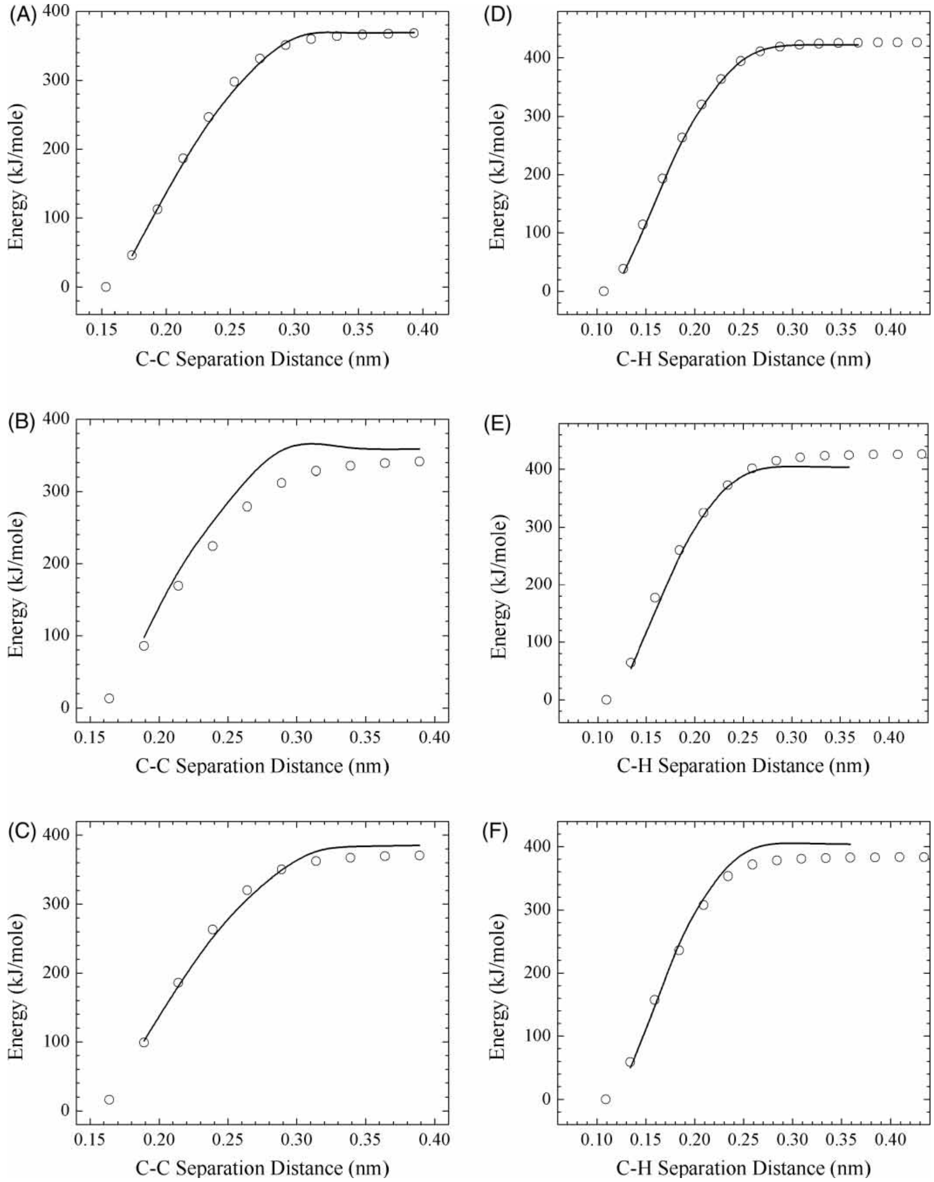

Figure 6. Comparison of the C—C scission reactive potential in (a) propane, (b) ethyl amine and (c) ethyl fluorine and of the C—H scission reactive potential in (d) methane, (e) methanol and (f) acetaldehyde.

radicals. The new method provides an accurate description of bond dissociations without the need for molecular-orbital bond-order calculations.

The new method provides an accurate description of bond dissociations without the need for molecular-orbital bond-order calculations. RMDff provides a flexible methodology for creating a smooth PES for a reactive potential. The use of equilibrium forcefields allows for the base of the reactive system to be developed from tested equilibrium forcefield models. The use of atom types allows for high specification in each reaction. The application of the switching functions then permits reactions to be developed in a straightforward manner connecting reactant and product descriptions in accurate, smooth PESs. Because reactions are relatively rare, the use of equilibrium forcefields as a basis for RMDff allows accurate results in the simulations in the nonreactive cases. Overall, RMDff provides a flexible method that can be easily used to design a representation of reactions using forcefields that have been previously developed and validated.

Acknowledgements

K. D. Smith and P. R. Westmoreland were supported through Cluster F of the Center for UMass-Industry Research on Polymers, a consortium sponsored by US Army, Boeing, DuPont, FAA, General Electric, Schneller, Solvay, NIST, Rogers, Johns Manville, Multina and International Association of Fire Fighters. The facility for some of the *ab initio* calculations were supported by the National Science Foundation under the following NSF programs: Partnerships for Advanced Computational Infrastructure, Distributed Terascale Facility (DTF) and Terascale Extensions: Enhancements to the Extensible Terascale Facility, whose support is appreciated.

A Appendix

Table A1. Definition of atom types used in table 1.

Atom type	*Description*
h	Hydrogen atom
cg	Generic sp^3 carbon
c	sp^3 carbon bonded to 4 heavy atoms
c1	sp^3 carbon bonded to 3 heavy atoms
c2	sp^3 carbon bonded to 2 heavy atoms
c3	sp^3 carbon bonded to 1 heavy atoms
c4	sp^3 carbon bonded to 0 heavy atoms
cf	Radical sp^2 carbon atom

References

[1] M.R. Nyden, G.P. Forney, J.E. Brown. Molecular modeling of polymer flammability: Application to the design of flame-resistant polyethylene. *Macromolecules*, **25**, 1658 (1992).

[2] M.R. Nyden, T.R. Coley, S. Mumby. Polystyrene. Application of molecular dynamics to the study of thermal degradation in aromatic polymers, Part I. *Polym. Eng. Sci.*, **37**, 1496 (1997).

[3] S.I. Stoliarov, P.R. Westmoreland, M.R. Nyden, G.P. Forney. A reactive molecular dynamics model of thermal decomposition in polymers: I. Poly(methyl methacrylate). *Polymer*, **44**, 883 (2003).

[4] M.R. Nyden, S.I. Stoliarov, P.R. Westmoreland, Z.X. Guo, C. Jee. Application of reactive molecular dynamics to the study of the thermal decomposition of polymers and nanoscale structures. *Mat. Sci. Eng. A Struct.*, **365**, 114 (2004).

[5] S.I. Stoliarov, R.E. Lyon, M.R. Nyden. A reactive molecular dynamics model of thermal decomposition in polymers: II. Polyisobutylene. *Polymer*, **45**, 8613 (2004).

[6] R. Car, M. Parrinello. Unified approach for molecular dynamics and density-functional theory. *Phys. Rev. Lett.*, **55**, 2471 (1985).

[7] M.E. Tuckerman, M. Parrinello. Integrating the Car-Parrinello equations. I. Basic integration techniques. *J. Chem. Phys.*, **101**, 1302 (1994).

[8] A.C.T. van Duin, S. Dasgupta, F. Lorant, W.A. Goddard III. ReaxFF: A reactive force field for hydrocarbons. *J. Phys. Chem. A*, **105**, 9396 (2001).

[9] A.C.T. van Duin, A. Strachan, S. Stewman, Q. Zhang, X. Xu, W.A. Goddard III. $\text{ReaxFF}_{\text{SiO}}$ reactive force field for silicon and silicon oxide systems. *J. Phys. Chem. A*, **107**, 3803 (2003).

[10] D.W. Brenner. Empirical potential for hydrocarbons for use in simulating the chemcial vapor deposition of diamond films. *Phys. Rev. B*, **42**, 9458 (1990).

[11] D.W. Brenner. Erratum: Empirical potential for hydrocarbons for use in simulating the chemcial vapor deposition of diamond films. *Phys. Rev. B*, **46**, 1948 (1992).

[12] S.J. Stuart, Y. Li, O. Kum, J.W. Mintmire, A.F. Voter. Reactive bond-order simulations using both spatial and temporal approaches to parallelism. *J. Chem. Phys.*, **112**, 6472 (2000).

[13] D.W. Brenner, O.A. Shenderova, J.A. Harrison, S.J. Stuart, B. Ni, S.B. Sinnott. A second-generation reactive empirical bond order (REBO) potential energy expression for hydrocarbons. *J. Phys. Condens. Mat.*, **14**, 783 (2002).

[14] J. Aqvist, A. Warshel. Simulation of enzyme reactions using valence bond force fields and other hybrid quantum/classical approaches. *Chem. Rev.*, **93**, 2523 (1993).

[15] A. Warshel, R.M. Weiss. An empirical valence bond approach for comparing reactions in solutions and in enzymes. *J. Am. Chem. Soc.*, **102**, 6218 (1980).

[16] F. Jensen, P. Norrby. Transition states from empirical force fields. *Theor. Chem. Acc.*, **109**, 1 (2003).

[17] Y. Kim, J.C. Corchado, J. Villa, J. Xing, D.G. Truhlar. Multiconfigurational molecular mechanics algorithm for potential energy surfaces of chemical reactions. *J. Chem. Phys.*, **112**, 2718 (2000).

[18] T.N. Truong. Reaction class transition state theory: Hydrogen abstraction reactions by hydrogen atoms as test cases. *J. Chem. Phys.*, **113**, 4957 (2000).

[19] N. Kungwan, T.N. Truong. Kinetics of the hydrogen abstraction $\bullet CH_3 + \text{Alkane} \rightarrow CH_4 + \text{Alkyl}$ reaction class: An application of the reaction class transition state theory. *J. Phys. Chem. A*, **109**, 7742 (2005).

[20] M.J. Frisch, G.W. Trucks, H.B. Schlegel, G.E. Scuseria, M.A. Robb, J.R. Cheeseman, V.G. Zakrzewski, J.A. Montgomery Jr., R.E. Stratmann, J.C. Burant, S. Dapprich, J.M. Millam, A.D. Daniels, K.N. Kudin, M.C. Strain, O. Farkas, J. Tomasi, V. Barone, M. Cossi, R. Cammi, B. Mennucci, C. Pomelli, C. Adamo, S. Clifford, J. Ochterski, G.A. Petersson, P.Y. Ayala, Q. Cui, K. Morokuma, D.K. Malick, A.D. Rabuck, K. Raghavachari, J.B. Foresman, J. Cioslowski, J.V. Ortiz, B.B. Stefanov, G. Liu, A. Liashenko, P. Piskorz, I. Komaromi, R. Gomperts, R.L. Martin, D.J. Fox, T. Keith, M.A. Al-Laham, C.Y. Peng, A. Nanayakkara, C. Gonzalez, M. Challacombe, P.M.W. Gill, B. Johnson, W. Chen, M.W. Wong, J.L. Andres, C. Gonzalez, M. Head-Gordon, E.S. Replogle, J.A. Pople. Gaussian 98, Revision A.7 and A.9, Gaussian, Inc., Pittsburgh, PA (1998).

[21] M.J. Frisch, G.W. Trucks, H.B. Schlegel, G.E. Scuseria, M.A. Robb, J.R. Cheeseman, J.A. Montgomery Jr., T. Vreven, K.N. Kudin, J.C. Burant, J.M. Millam, S.S. Iyengar, J. Tomasi, V. Barone, B. Mennucci, M. Cossi, G. Scalmani, N. Rega, G.A. Petersson, H. Nakatsuji, M. Hada, M. Ehara, K. Toyota, R. Fukuda, J. Hasegawa, M. Ishida, T. Nakajima, Y. Honda, O. Kitao, H. Nakai, M. Klene, X. Li, J.E. Knox, H.P. Hratchian, J.B. Cross, V. Bakken, C. Adamo, J. Jaramillo, R. Gomperts, R.E. Stratmann, O. Yazyev, A.J. Austin, R. Cammi, C. Pomelli, J.W. Ochterski, P.Y. Ayala, K. Morokuma, G.A. Voth, P. Salvador, J.J. Dannenberg, V.G. Zakrzewski, S. Dapprich,

A.D. Daniels, M.C. Strain, O. Farkas, D.K. Malick, A.D. Rabuck, K. Raghavachari, J.B. Foresman, J.V. Ortiz, Q. Cui, A.G. Baboul, S. Clifford, J. Cioslowski, B.B. Stefanov, G. Liu, A. Liashenko, P. Piskorz, I. Komaromi, R.L. Martin, D.J. Fox, T. Keith, M.A. Al-Laham, C.Y. Peng, A. Nanayakkara, M. Challacombe, P.M.W. Gill, B. Johnson, W. Chen, M.W. Wong, C. Gonzalez, J.A. Pople. Gaussian 03, Revision C.02 and Gaussian Development Version, Revision D.02, Gaussian, Inc., Wallingford, CT (2004).

[22] S.F. Boys, F. Bernardi. Calculation of small molecular interactions by differences of separate total energies. Some procedures with reduced error. *Mol. Phys.*, **19**, 553 (1970).

[23] N.L. Allinger, Y.H. Yul, J. Lii. Molecular mechanics. The MM3 force field for hydrocarbons. 1. *J. Am. Chem. Soc.*, **111**, 8552 (1989).

[24] J. Lii, N.L. Allinger. Molecular mechanics. The MM3 force field for hydrocarbons. 3. The van der Waals potentials and crystal data for aliphatic and aromatic hydrocarbons. *J. Am. Chem. Soc.*, **111**, 8576 (1989).

[25] J. Lii, N.L. Allinger. Molecular mechanics. The MM3 force field for hydrocarbons. 2. Vibrational frequencies and thermodynamics. *J. Am. Chem. Soc.*, **111**, 8566 (1989).

[26] K. Gundertofte, T. Lilefors, N. Per-Ola, I. Pettersson. A comparison of conformational energies calculated by several molecular mechanics methods. *J. Comput. Chem.*, **17**, 429 (1996).

[27] C.A. Stortz. Comparative Performance of MM3(92) and two TINKER MM3 versions for the modeling of carbohydrates. *J. Comput. Chem.*, **26**, 471 (2005).

[28] S.E. Feller, A.D. MacKerell Jr. An improved empirical potential energy function for molecular simulations of phospholipids. *J. Phys. Chem. B*, **104**, 7510 (2000).

[29] S. Tsuzuki, T. Uchimaru, K. Tanabe, S. Kuwajima. Refinement of nonbonding interaction potential parameters for methane on the basis of the pair potential obtained by MP3/6-311G(3d,3p)-level *ab Initio* molecular orbital calculations: Anisotropy of H/H Interaction. *J. Phys. Chem.*, **98**, 1830 (1994).

[30] G. Kaminski, E.M. Duffy, T. Matsui, W.L. Jorgensen. Free energies of hydration and pure liquid properties of hydrocarbons from the OLPS all-atom model. *J. Phys. Chem.*, **98**, 13077 (1994).

[31] D.F. McMillen, D.M. Golden. Hydrocarbon bond dissociation energies. *Ann. Rev. Phys. Chem.*, **33**, 493 (1982).

[32] J.W.M. Carneiro, J.F. Dias, J.G.R. Tostes, P.R. Seidl, A. Taft. Hyperconjugation effects of hydroxyl and amine groups on chemical shifts of neighboring carbon nuclei. *Int. J. Quantum Chem.*, **95**, 322 (2003).